Journal of Applied Mathematics and Mechanics

ZAMM

Zeitschrift für Angewandte Mathematik und Mechanik
Founded by Richard von Mises in 1921

www.zamm-journal.org

WILEY

ZAMM · Z. Angew. Math. Mech. **96**, No. 12, 1457–1466 (2016) / **DOI** 10.1002/zamm.201500266

On fully developed mixed convection with viscous dissipation in a vertical channel and its stability

A. Barletta[1],* **and M. Miklavčič**[2],**

[1] Department of Industrial Engineering, Alma Mater Studiorum Università di Bologna, Viale Risorgimento 2, 40136 Bologna, Italy
[2] Department of Mathematics, Michigan State University, E. Lansing, MI 48824, USA

Received 26 October 2015, accepted 28 May 2016
Published online 4 July 2016

Key words Convective instability, mixed convection, viscous dissipation.

The fully developed regime of mixed convection in a vertical plane channel with symmetric and uniform temperature prescribed on the bounding walls is studied. The effect of viscous dissipation is taken into account and the Oberbeck-Boussinesq approximation is adopted by choosing the average fluid temperature as the reference temperature. The viscous dissipation effect induces the existence of dual branches of stationary solutions. A nonlinear stability analysis versus fully-developed modes of perturbation is carried out showing that the second branch of dual stationary solutions is unstable.

1 Introduction

The fully developed buoyant flow in a vertical channel has been widely investigated by several authors in the last decades [1–4]. The general case of combined forced and free convection has been studied by considering either isothermal channel walls or walls subject to a uniform heat flux. When the flow regime is free convection, the net mass flow rate across the channel vanishes. In this special regime and for a vertical parallel plane channel, the linear instability of the basic velocity profile, given by a cubic polynomial function of the horizontal coordinate, was studied by Gill and Davey [5], Vest and Arpaci [6], Korpela et al. [7], and more recently by McBain and Armfield [8].

Further studies on the fully developed mixed convection in a vertical parallel channel were carried out by including the effect of viscous dissipation [9–13]. In particular, Barletta et al. [10–12] and Miklavčič and Wang [13] pointed out that the effect of viscous dissipation yields the existence of dual solutions of the governing equations corresponding either to a prescribed pressure gradient or to a prescribed mass flow rate. The two distinct branches of fully-developed solutions exist and satisfy the externally imposed constraints, namely the boundary conditions and the input data (the given pressure gradient, or the given mass flow rate). Stability analyses of the dual solutions emerging in viscous dissipation buoyant flows are quite rare in the literature. Besides the analysis by Barletta and Rees [14], relative to a fluid saturated horizontal porous channel, the only study dealing with the stability of dual buoyant flows with viscous dissipation in a vertical channel is that recently published by Miklavčič [15]. This paper presents a nonlinear stability analysis focusing on special modes of perturbation preserving the parallel velocity, or fully-developed, flow regime. Although not general, this method of analysis has the valuable advantage of providing a proof that the second branch of dual solutions is unstable. The author considers a vertical plane channel where no temperature difference between the boundaries is prescribed, so that the viscous dissipation is the unique source of the buoyancy force and, thus, of the thermal instability. The governing equations analyzed by Miklavčič [15] are based on the Oberbeck-Boussinesq approximation [16] where the constrained wall temperature is taken as the reference temperature for the linearization of the fluid equation of state. Although being the simplest choice to carry out the analysis, the physical model behind this choice can lead to increasingly large errors when the internal heat input provided by the viscous dissipation is large enough. As pointed out by Barletta and Zanchini [4], the optimal choice of the reference temperature within the Oberbeck-Boussinesq approximation of buoyant flows is the average temperature evaluated over the fluid flow domain.

The aim of our contribution is to reconsider the analysis carried out by Miklavčič [15], in order to estimate the extent to which a different choice of the reference temperature in the formulation of the Oberbeck-Boussinesq approximation can influence the dual solutions for the basic flow, as well as the results of the stability analysis. In particular, the recommendation

* Corresponding author E-mail: antonio.barletta@unibo.it
** E-mail: milan@math.msu.edu

expressed and motivated by Barletta and Zanchini [4], to take the average fluid temperature as the reference temperature, is adopted in our study.

2 Mathematical model

Let us assume fully developed flow in a vertical channel defined by the domain $-L \leqslant y \leqslant L$. Here, $\mathbf{g} = -g\,\mathbf{e}_z$ is the gravitational acceleration with modulus g, and $\mathbf{e}_z$ is the unit vector along the vertical z-axis. The flow is driven by a constant vertical pressure gradient $P = \partial p/\partial z$ and by the buoyancy force induced by the temperature gradient. Fully developed regime means a velocity field parallel to the z-axis and expressed by its z-component W. Thus, the local momentum balance equation and the local energy balance equations formulated through the Oberbeck-Boussinesq approximation [4, 16] are given by

$$\rho\,\frac{\partial W}{\partial t} = \mu\,\frac{\partial^2 W}{\partial y^2} - P + \rho g\beta\,(T - T_m)\,, \tag{1a}$$

$$\rho c\,\frac{\partial T}{\partial t} = k\,\frac{\partial^2 T}{\partial y^2} + \mu\left(\frac{\partial W}{\partial y}\right)^2, \tag{1b}$$

while the boundary conditions are

$$y = \pm L: \qquad W = 0, \quad T = T_0. \tag{2}$$

In Eqs. (1) and (2), T stands for temperature and t for time. The density ρ, coefficient of thermal expansion β, specific heat c, thermal conductivity k, dynamic viscosity μ are fluid properties evaluated at the average temperature,

$$T_m = \frac{1}{2L}\int_{-L}^{L} T\,dy. \tag{3}$$

Strictly speaking, T_m is a function of time, so that also ρ, β, c, k, and μ should depend on time instead of being constant. However, coherently with the Oberbeck-Boussinesq approximation, all these quantities are expected to depend very weakly on T_m, so that they will be effectively supposed to be constant in the forthcoming computations.

2.1 Dimensionless equations

Equations (1) and (2) can be written in a dimensionless form by scaling the dimensional quantities as follows:

$$\frac{y}{L} \to y, \quad \frac{t}{L^2\rho/\mu} \to t, \quad \frac{W}{k/(\rho g\beta L^2)} \to W, \quad \frac{T - T_m}{k\mu/(\rho g\beta L^2)^2} \to T, \quad \frac{T_0 - T_m}{k\mu/(\rho g\beta L^2)^2} \to T_0,$$
$$\frac{P}{k\mu/(\rho g\beta L^4)} \to P. \tag{4}$$

In general, T_0 is a function of time. With this scaling, Eqs. (1)–(3) can be rewritten as

$$\frac{\partial W}{\partial t} = \frac{\partial^2 W}{\partial y^2} - P + T, \tag{5a}$$

$$\mathrm{Pr}\left(\frac{\partial T}{\partial t} - \frac{\mathrm{d}T_0}{\mathrm{d}t}\right) = \frac{\partial^2 T}{\partial y^2} + \left(\frac{\partial W}{\partial y}\right)^2, \tag{5b}$$

with the boundary conditions and additional integral constraint given by

$$y = \pm 1: \qquad W = 0, \quad T = T_0, \tag{6a}$$

$$\int_{-1}^{1} T\,dy = 0. \tag{6b}$$

The Prandtl number, employed in Eq. (5b), is defined as

$$\mathrm{Pr} = \frac{c\mu}{k}. \tag{7}$$

2.2 Stationary basic flows

Assuming stationary flow, Eqs. (5) become ordinary differential equations,

$$W'' - P + T = 0, \tag{8a}$$

$$T'' + (W')^2 = 0, \tag{8b}$$

where primes denote derivatives with respect to y. Equations (8), together with Eqs. (6), can be solved numerically for a fixed input value of P. We mention that T_0 is a constant, in this case, and it needs not be fixed a-priori as its value is determined so that the integral constraint (6b) is satisfied. Even solutions of Eq. (8),

$$W(-y) = W(y), \quad T(-y) = T(y), \quad \forall y \in [-1, 1], \tag{9}$$

are sought. They satisfy the midplane conditions

$$W'(0) = 0, \quad T'(0) = 0. \tag{10}$$

Moreover, on account of Eqs. (6b) and (8a), even solutions are constrained by the condition

$$W'(-1) = -W'(1) = -P. \tag{11}$$

Even solutions can be determined by solving numerically Eqs. (8) for $y \in [0, 1]$ with the boundary conditions

$$W'(0) = 0, \quad T'(0) = 0, \quad W(1) = 0, \quad W'(1) = P. \tag{12}$$

The resulting boundary value problem, Eqs. (8) and (12), depends only on the input parameter P. When the numerical solution of Eqs. (8) and (12) is obtained, T_0 can be evaluated by using the condition (6a), namely

$$T_0 = T(1). \tag{13}$$

Another important quantity to be defined is the average dimensionless velocity which, for even solutions, is given by

$$W_m = \frac{1}{2}\int_{-1}^{1} W\, dy = \int_{0}^{1} W\, dy. \tag{14}$$

For a prescribed value of $P \geqslant -17.128$, two solutions are allowed, thus defining a first and a second branch. The dual solutions coincide when $P = -17.128$, while no solutions exist if $P < -17.128$. Plots of the parametric conditions leading to solutions of Eqs. (8) and (12) are reported in Fig. 1. In this figure, points A, B, C, D, E, F, G correspond to special flow conditions and are given by

$$\mathrm{A}: \quad P = 0, \quad W(0) = 0, \quad T_0 = 0, \quad W_m = 0, \tag{15a}$$

$$\mathrm{B}: \quad P = -17.128, \quad W(0) = 14.936, \quad T_0 = -68.510, \quad W_m = 9.3132, \tag{15b}$$

$$\mathrm{C}: \quad P = 0, \quad W(0) = 24.847, \quad T_0 = -241.02, \quad W_m = 13.906, \tag{15c}$$

$$\mathrm{D}: \quad P = 14.258, \quad W(0) = 26.961, \quad T_0 = -320.62, \quad W_m = 14.258, \tag{15d}$$

$$\mathrm{E}: \quad P = 57.543, \quad W(0) = 28.772, \quad T_0 = -516.48, \quad W_m = 12.693 \tag{15e}$$

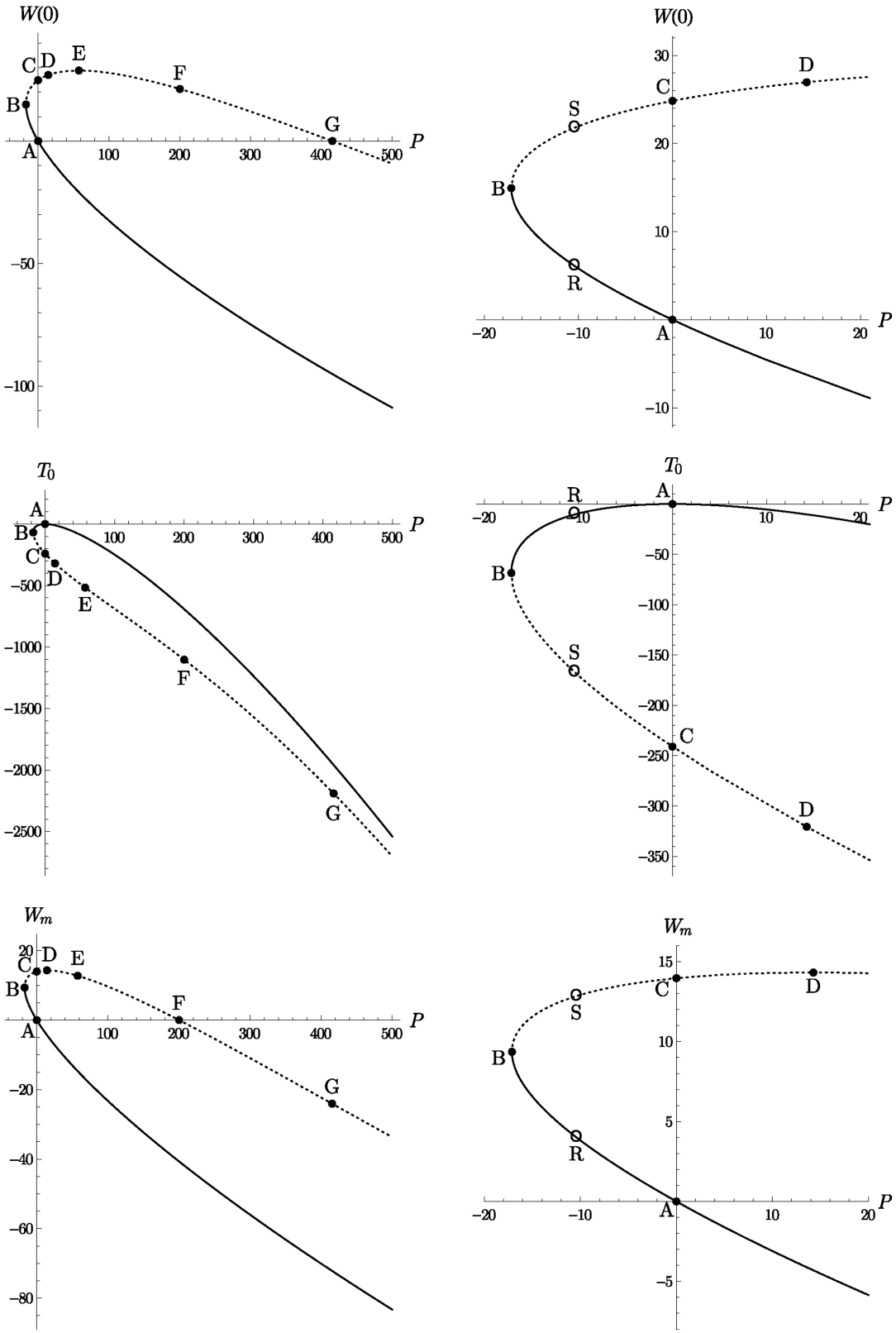

Fig. 1 Dual basic solutions: first branch (solid line) and second branch (dotted line). Points A, B, C, D, E, F, G, R, S correspond to special flows discussed below.

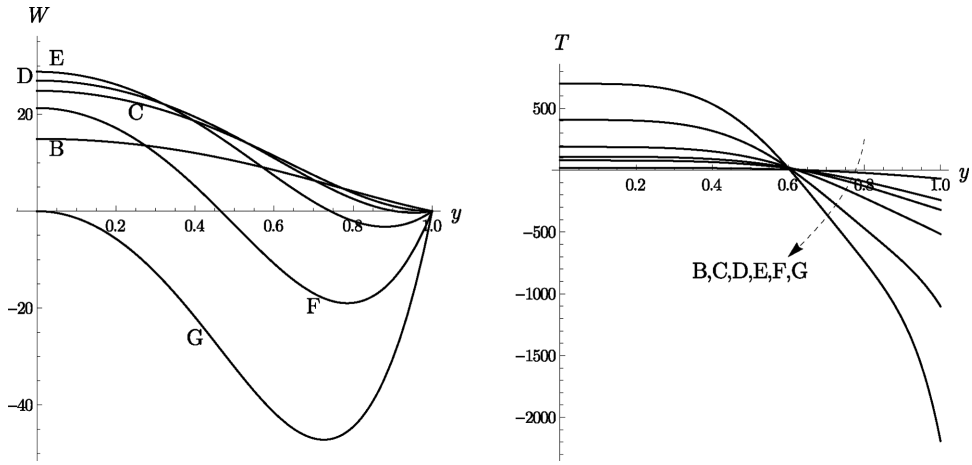

Fig. 2 Dual basic solutions: plots of $W(y)$ and $T(y)$ for the parametric conditions B, C, D, E, F, G defined by Eqs. (15).

$$\text{F}: \qquad P = 199.81, \quad W(0) = 21.299, \quad T_0 = -1101.2, \quad W_m = 0 \tag{15f}$$

$$\text{G}: \qquad P = 415.42, \quad W(0) = 0, \quad T_0 = -2191.3, \quad W_m = -24.066. \tag{15g}$$

Point A defines the trivial solution of Eqs. (8) and (12) where $W = 0$ and $T = 0$. Point B corresponds to the coincident dual solutions occurring at the minimum value of P. Point C is the completely passive convection solution. Point D describes the solution where the average velocity W_m is at its maximum. Point E defines the flow where the midplane velocity $W(0)$ is at its maximum. Point F describes the nontrivial flow conditions where the average velocity W_m vanishes. Finally, point G yields the nontrivial solution with $W(0) = 0$.

Figure 2 displays plots of $W(y)$ and $T(y)$ for the parametric conditions defined by Eqs. (15).

The flow called completely passive natural convection by Miklavčič and Wang [13] has velocity profile that is identical to the velocity profile corresponding to the flow marked by R on Fig. 1, in particular, $W(0) = 6.1114$. Miklavčič and Wang [13] called the flow completely passive because because in their model $P = 0$, however, our current model requires pressure gradient $P = -10.41449$ to maintain this velocity profile. This velocity profile does not have an inflection point, but flows with $W(0) > 6.1114$ have an inflection point. The flow with the same pressure gradient $P = -10.41449$, but on the second branch, is denoted by S on Fig. 1 and has $W(0) = 21.7931$. These two flows will be used to illustrate stability results in the next two sections.

3 Stability analysis

Let (W, T, T_0) be any basic flow defined by the stationary even solution discussed in Sect. 2.2. Perturbations of the basic flow are defined so that they reflect the fully developed regime, namely

$$W(y) + u_1(y,t), \quad T(y) + \theta(y,t), \quad T_0 + \theta_0(t). \tag{16}$$

We mention that (u_1, θ, θ_0) are perturbations of a special type, while a general disturbance of the basic flow should be three-dimensional. However, analysis of the perturbations defined by Eq. (16) is sufficient to establish some basic features about the instability of the second branch of basic flow solutions.

On account of Eq. (16), the dynamics of the perturbations is obtained by Eqs. (5) which can be rewritten as

$$\frac{\partial u_1}{\partial t} = \frac{\partial^2 u_1}{\partial y^2} + \theta, \tag{17a}$$

$$\text{Pr}\left(\frac{\partial \theta}{\partial t} - \frac{\mathrm{d}\theta_0}{\mathrm{d}t}\right) = \frac{\partial^2 \theta}{\partial y^2} + 2\,\frac{\partial u_1}{\partial y}\,W' + \left(\frac{\partial u_1}{\partial y}\right)^2, \tag{17b}$$

while Eqs. (6) yield

$$y = \pm 1 : \qquad u_1 = 0, \quad \theta = \theta_0, \tag{18a}$$

$$\int_{-1}^{1} \theta \, dy = 0. \tag{18b}$$

Let us define

$$u_2(y,t) = \theta(y,t) - \theta_0(t). \tag{19}$$

Then, Eqs. (17) and (18a) can be rewritten as

$$\frac{\partial u_1}{\partial t} = \frac{\partial^2 u_1}{\partial y^2} + u_2 - \frac{1}{2}\int_{-1}^{1} u_2 \, dy, \tag{20a}$$

$$\mathrm{Pr}\,\frac{\partial u_2}{\partial t} = \frac{\partial^2 u_2}{\partial y^2} + 2\,\frac{\partial u_1}{\partial y}\,W' + \left(\frac{\partial u_1}{\partial y}\right)^2, \tag{20b}$$

$$y = \pm 1 : \qquad u_1 = 0, \quad u_2 = 0. \tag{20c}$$

This system can be considered as an abstract evolution equation

$$\frac{\partial u}{\partial t} + Au = f(u) \tag{21}$$

of $u = (u_1, u_2)$ in $(L^2(-1,1))^2$ where the linear operator A is given by

$$(Au)_1 = -u_1'' - u_2 + \frac{1}{2}\int_{-1}^{1} u_2 dy, \qquad (Au)_2 = (-u_2'' - 2W'u_1')/\mathrm{Pr} \tag{22}$$

with the domain $D(A) = (W_0^1(-1,1) \cap W^2(-1,1))^2$ and

$$f(u)_1 = 0, \qquad f(u)_2 = (u_1')^2/\mathrm{Pr}. \tag{23}$$

One can prove that (21) is a semilinear parabolic equation [17] and that A has compact resolvent. Hence the well known stability theory for semilinear parabolic equations, see for example Miklavčič [17], can be applied to show that (nonlinear) stability of stationary solutions w, θ is determined by the eigenvalues of A. $-\lambda$ is an eigenvalue of A iff there exists a nontrivial solution of

$$\lambda\, v = v'' + \tau - \frac{1}{2}\int_{-1}^{1} \tau dy \tag{24}$$

$$\mathrm{Pr}\,\lambda\,\tau = \tau'' + 2W'v' \tag{25}$$

$$v = \tau = 0 \quad \text{at } y = \pm 1. \tag{26}$$

In this notation, if every eigenvalue λ has negative real part then all small perturbations of the stationary solution decay (p. 265 in [17]). If on the other hand at least one eigenvalue has positive real part then one can find arbitrarily small perturbations of the stationary solution that eventually become larger than a fixed threshold (p. 266 in [17]).

The obvious central difference approximations were used to discretize (24), (25) and then the eigenvalues of the corresponding matrix were calculated. Richardson extrapolation, using two discretizations, was used to improve accuracy.

The trivial solution at the point A on Fig. 1 has $W = 0$ and the corresponding eigenvalues of the system (24)–(26) are equal to

$$-(n\pi/2)^2, \quad -(n\pi/2)^2/\mathrm{Pr} \quad \text{where } n = 1, 2, \ldots \tag{27}$$

- just like in Miklavčič [15]. Hence the trivial solution is stable. When $1/4 < \mathrm{Pr} < 4$ the leading eigenvalues are $-(\pi/2)^2$ and $-(\pi/2)^2/\mathrm{Pr}$. As $W(0)$ decreases from 0, i.e. moving to the right of 0 on the first branch of Fig. 1, they merge and then form a complex conjugate pair with slowly varying real part. As $W(0)$ increases i.e. moving up from 0 on Fig. 1, the

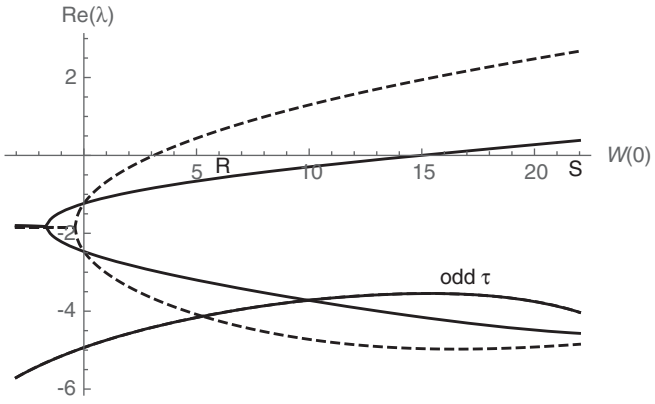

Fig. 3 The solid curves show the real parts of three of the largest eigenvalues when $\mathrm{Pr} = 2$. The dashed curves show the two leading eigenvalues for the corresponding system in Miklavčič [15].

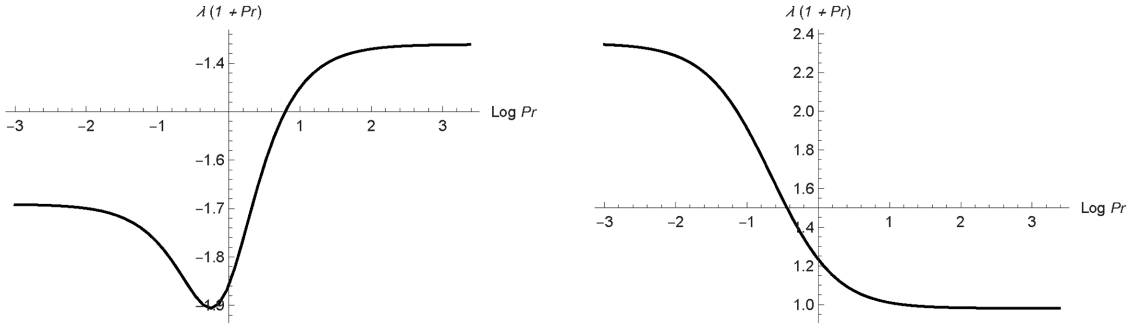

Fig. 4 Dependence of the leading eigenvalue for the flows R (left) and S on the Prandtl number.

eigenvalues separate more and the leading one changes the sign at exactly the turning point B on Fig. 1. When $\mathrm{Pr} = 2$, the leading three eigenvalues are presented on Fig. 3. For comparison the leading eigenvalues obtained in Miklavčič [15] are presented by the dashed curve. The eigenfunctions τ corresponding to the eigenvalues on the curve labeled "odd τ" are odd, hence the average in Eq. (24) is 0, and therefore the eigenvalues on the curve labeled "odd τ" are also eigenvalues for the system in Miklavčič [15].

The argument showing that stability changes at exactly the turning point B is exactly the same as in Miklavčič [15]. In particular, the point of change of stability does not depend on the Prandtl number. The effect of Pr on the eigenvalues is demonstrated on Fig. 4.

Note that our model predicts that the change of stability occurs when $W(0) = 14.9$. On the other hand the model in Miklavčič [15] predicts that the change of stability occurs when $W(0) = 3.1$. The completely passive convection flow in Miklavčič and Wang [13] has $W(0) = 6.1$, hence it is stable according to the current dynamic model and unstable according to the dynamic model in Miklavčič [15].

Since the maximum value of $W(0)$ is reached on the second branch, see Fig. 1, it makes more sense to use P as a parameter in presentation of eigenvalues on the second branch. See Fig. 5. Calculations were done for P past 300 and no change in trends was observed. The leading eigenvalue is simply increasing with P which makes all stationary solutions on the second branch in Fig. 1 unstable. We expect that any perturbation of a stationary solution on the second branch evolves over time into the stable solution on the first branch at the same P. An example is given in the next section.

In Barletta et al. [10] solutions were characterized with a parameter Ξ which is 16 times the average velocity W_m, Eq. (14),

$$\Xi = 16\, W_m = 16 \int_0^1 W(y)\, dy. \tag{28}$$

From Eq. (15d), the maximum value Ξ can obtain is, 228.13 (in agreement with Barletta et al. [10]) and occurs with $W(0) = 26.961$ in the second branch on Fig. 1. For each value less than the maximum value of Ξ, Barletta et al. [10] found dual stationary solutions with the same average velocity. One of them is to the right of the point where maximum Ξ occurs, hence is always unstable, and the other one is the left of the point - possibly on the first branch. From Eq. (15b), at the turning point B we have $\Xi_T = 149.01$. Hence when $\Xi > \Xi_T$ both dual solutions are unstable and when $\Xi < \Xi_T$ one of the dual solutions is stable and one unstable. The model in Miklavčič [15] predicts the same but with the value of $\Xi_T = 32.7$.

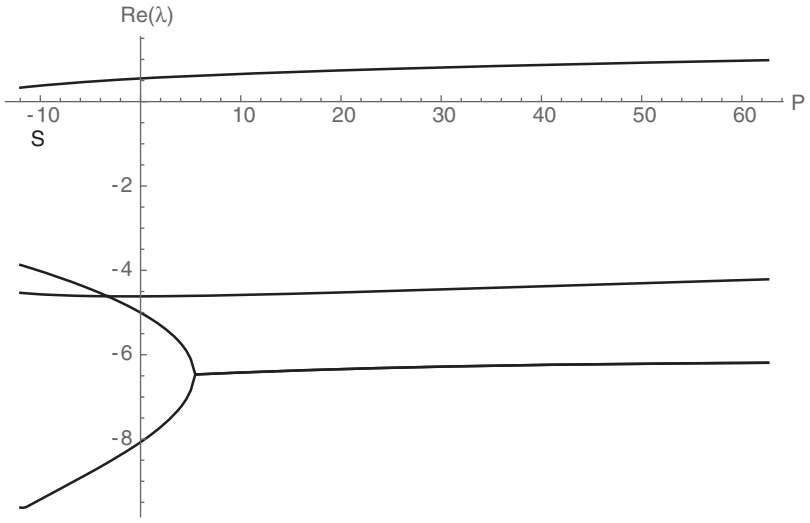

Fig. 5 Real parts of four of the largest eigenvalues when $\mathrm{Pr} = 2$ on the second branch of Fig. 1.

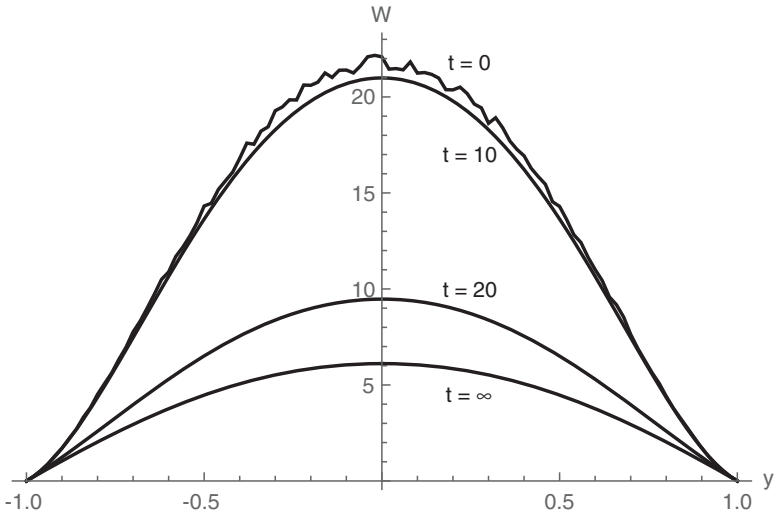

Fig. 6 Evolution of the velocity W.

4 Direct simulation

Here we present an example of an evolution of a slightly perturbed flow on the second branch of Fig. 1 by solving Eqs. (5), (6) numerically. We chose to do this at $P = -10.41449$ and $\mathrm{Pr} = 2$. The flow with this P on the second branch is marked by S on Fig. 1 and its leading eigenvalue is equal to 0.3731. Its dual flow R on the first branch has the leading eigenvalue equal to -0.5697. The corresponding velocity profiles are denoted by W_S and W_R.

We perturbed the velocity and temperature at $n = 99$ equally spaced points y_i between -1 and 1 by random amounts within $\pm 2\%$ of the stationary values. The top curve on Fig. 6 shows the initial velocity distribution and is close to W_S. Note that it is slightly asymmetric to allow for possibility of evolution towards a non symmetric solution. We solved Eqs. (5), (6) by the finite difference method. The middle two curves on Fig. 6 show the velocity distribution at $t = 10$ and $t = 20$. The size of the perturbation was calculated as follows

$$\frac{1}{n}\sqrt{\sum_{i=1}^{n}(W(y_i,t) - W_\mathrm{S}(y_i))^2}$$

and is plotted on Fig. 7. Near $t = 8$ the perturbation is still small, hence linearization makes sense, and since the perturbation has been evolving for some time, one would expect that the projection on the leading eigenvector is the dominant part of the perturbation. From the data at $t = 8$ and 8.1 we calculated the actual growth rate to be 0.382, which is not too far

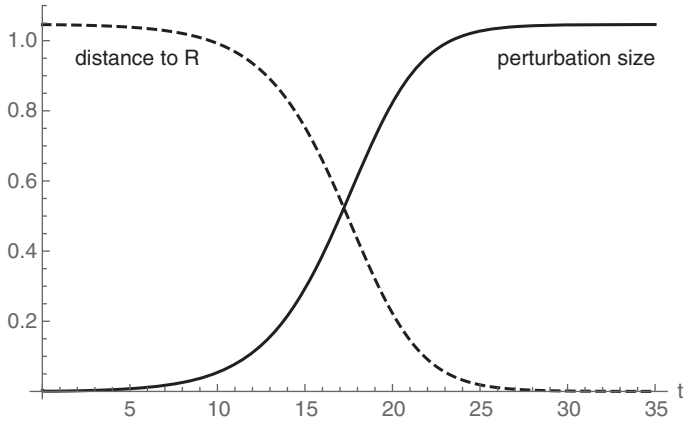

Fig. 7 Growth of a perturbation of S and its approach to flow R.

from the leading eigenvalue 0.3731. Note that the initial actual growth rate depends on the initial perturbation and on the discretization size n.

We expected that the perturbed flow will evolve toward flow R whose velocity profile W_{R} is represented by the bottom curve on Fig. 6. In order to confirm our expectation we calculated

$$\frac{1}{n}\sqrt{\sum_{i=1}^{n}(W(y_i,t)-W_{\mathrm{R}}(y_i))^2}$$

and presented results on Fig. 7 with a dashed curve. From the data for Fig. 7 we determined the actual decay rate between $t = 26$ and 26.1 to be -0.556 which is a good approximation of the leading eigenvalue -0.5697. The actual decay rate depends on n and a bit on initial perturbation.

5 Conclusions

The local balance equations for the fully developed mixed convection flow in a vertical channel, with both boundary walls kept at a fixed ambient temperature, are formulated according to the Oberbeck-Boussinesq approximation, using the average fluid temperature as the reference temperature, and not neglecting the effect of viscous dissipation.

We employed the theory of semilinear parabolic equations to investigate stability of flows and we also did some direct simulation of evolution of flows. The overall picture of dynamics is similar to the one presented by Miklavčič [15] using the fixed ambient temperature as a reference temperature, however, details are strikingly different. Here are three examples:

1) In both cases, the pressure gradient needs to exceed a certain negative threshold value for existence of stationary solutions. At each pressure gradient that exceeds the threshold value both models give dual stationary solutions. The branch with lower velocity is stable and the other one is unstable. However, the threshold value is over 5 times bigger in our model then in the model using fixed ambient temperature as a reference temperature.

2) In both cases, the same velocity profiles are allowed, and when the velocity in the center reaches a certain positive value the flow loses stability. This happens at almost 5 times bigger velocities when using the average fluid temperature as the reference temperature compared to when using the fixed ambient temperature as the reference temperature. This transition happens at the threshold pressure gradient.

3) The velocity profile called completely passive natural convection by Miklavčič and Wang [13] is unstable when using the fixed ambient temperature as the reference temperature, however, in our model it is stable. Moreover, direct simulations using our nonlinear time dependent model show that it actually attracts evolving flows that are under the same pressure gradient as is required for its existence.

In view of the differences like above it is time for experimentalists to voice their opinion.

References

[1] W. Aung and G. Worku, Theory of fully developed, combined convection including flow reversal, J. Heat Transf. **108**, 485–488 (1986).

[2] T. T. Hamadah and R. A. Wirtz, Analysis of laminar fully developed mixed convection in a vertical channel with opposing buoyancy, J. Heat Transf. **113**, 507–510 (1991).
[3] G. D. McBain, Fully developed laminar buoyant flow in vertical cavities and ducts of bounded section, J. Fluid Mech. **401**, 365–377 (1999).
[4] A. Barletta and E. Zanchini, On the choice of the reference temperature for fully-developed mixed convection in a vertical channel, Int. J. Heat Mass Transf. **42**, 3169–3181 (1999).
[5] A. E. Gill and A. Davey, Instabilities of a buoyancy-driven system, J. Fluid Mech. **35**, 775–798 (1969).
[6] C. M. Vest and V. S. Arpaci, Stability of natural convection in a vertical slot, J. Fluid Mech. **36**, 1–15 (1969).
[7] S. A. Korpela, D. Gözüm, and C. B. Baxi, On the stability of the conduction regime of natural convection in a vertical slot, Int. J. Heat Mass Transf. **16**, 1683–1690 (1973).
[8] G. D. McBain and S. W. Armfield, Natural convection in a vertical slot: accurate solution of the linear stability equations, The ANZIAM Journal **45**, C92–C105 (2004) .
[9] A. Barletta, Laminar mixed convection with viscous dissipation in a vertical channel, Int. J. Heat Mass Transf. **41**, 3501–3513 (1998).
[10] A. Barletta, E. Magyari, and B. Keller, Dual mixed convection flows in a vertical channel, Int. J. Heat Mass Transf. **48**, 4835–4845 (2005) .
[11] A. Barletta, E. Magyari, I. Pop, and L. Storesletten, Mixed convection with viscous dissipation in a vertical channel filled with a porous medium, Acta Mech. **194**, 123–140 (2007).
[12] A. Barletta, S. Lazzari, and E. Magyari, Buoyant Poiseuille-Couette flow with viscous dissipation in a vertical channel, Z. Angew. Math. Phys. **59**, 1039–1056 (2008).
[13] M. Miklavčič and C. Y. Wang, Completely passive natural convection, ZAMM-J. Appl. Math. Mech./Z. Angew. Math. Mech. **91**, 601–606 (2011).
[14] A. Barletta and D. A. S. Rees, Stability analysis of dual adiabatic flows in a horizontal porous layer, Int. J. Heat Mass Transf. **52**, 2300–2310 (2009).
[15] M. Miklavčič, Stability analysis of some fully developed mixed convection flows in a vertical channel, ZAMM-J. Appl. Math. Mech./Z. Angew. Math. Mech. **95**, 982–986 (2015).
[16] A. Barletta, Local energy balance, specific heats and the Oberbeck-Boussinesq approximation, Int. J. Heat Mass Transf. **52**, 5266–5270 (2009) .
[17] M. Miklavčič, Applied Functional Analysis and Partial Differential Equations (World Scientific Publishing Co. Inc., River Edge, NJ, 1998).

